Deformation defects and electron irradiation effect in a nanostructured Al–Mg aluminum alloy processed by severe plastic deformation

LIU Man-ping[1,2]*, SUN Shao-chun[1], Hans J. ROVEN[2],
Yingda YU[2], ZHANG Zhen[1], Maxim MURASHKIN[3], Ruslan Z. VALIEV[3]

1. School of Materials Science and Engineering, Jiangsu University, Zhenjiang 212013, China
2. Department of Materials Science and Engineering,
Norwegian University of Science and Technology (NTNU), Trondheim 7491, Norway
3. Institute of Physics of Advanced Materials, Ufa State Aviation Technical University, Ufa 450000, Russia

Abstract: In order to explore the exact nature of deformation defects previously observed in nanostructured Al-Mg alloys subjected to severe plastic deformation, a more thorough examination of the radiation effect on the formation of the planar defects in the high pressure torsion (HPT) alloys was conducted in this paper using high-resolution transmission electron microscopy (HRTEM). The results show that high densities of the defects in the HRTEM images disappear completely when these images expose under the electron beam for some duration of time. At the same time, lattice defects are never been observed within no-defect areas even when the beam-exposure increases to the degree that holes appear in the areas. Therefore, the HRTEM examinations confirm that the planar defects observed in the HPT alloys are mainly resulted from the significant plastic deformation and are not due to the radiation effect during HRTEM observation.

Key words: Al–Mg aluminum alloy; severe plastic deformation; high pressure torsion; electron irradiation; deformation defects; transmission electron microscopy

1 Introduction

It is well established that bulk nanostructured materials (BNM) can be produced successfully via microstructural refinement using severe plastic deformation (SPD), i.e. heavy straining under high imposed pressure [1–6]. SPD processing is an attractive procedure for many advanced applications, as it allows enhancing significantly properties of commonly used metals and alloys [2–4]. High pressure torsion (HPT) is one of the most promising SPD techniques because it has the potential to produce nanostructures with grain sizes of less than 100 nm [5–6]. Although outstanding progress has been made in this area in recent years, genesis of the structural features in SPD-processed metals is not yet fully understood [6–12]. In our previous works, deformation defects such as full and partial dislocations, dipoles, microtwins and stacking faults (SFs) have been frequently observed using transmission electron microscopy (TEM) and high-resolution TEM (HRTEM) in nanostructured Al-Mg alloys subjected to HPT [13–19]. However some reports argue that such lattice defects along the {111} planes in Al and Al based alloys often form (and may disappear) due to the irradiation effect during HRTEM observation [20–28]. In order to explore the exact

Foundation item: Project (50971087) supported by the National Natural Science Foundation of China; Project (SBK201222201) supported by the Basic Research Program (Natural Science Foundation) of Jiangsu Province); Project (10371800) supported by the Research Council of Norway under the NEW Light (NEWLIGHT) Metals of the Strategic Area (SA) Materials; Project (11JDG070) supported by the Senior Talent Research Foundation of Jiangsu University
Corresponding author: LIU Man-ping; E-mail: manping-liu@263.net; manpingliu@ujs.edu.cn

nature of these defects, a more thorough examination of the radiation effect on the formation of the planar defects in the HPT alloy was conducted in this paper.

2 Experimental

A commercial AA5182 Al–Mg alloy (Al-4.1Mg-0.35Mn-0.13Si-0.32Fe, by wt.%) received in the as-cast and homogenized condition were subjected to HPT to five turns with a rotation speed of 1 rpm under pressure of 6 GPa at room temperature. The calculated equivalent strain at the outer edge of the HPT samples is about 906 [2]. The deformed HPT samples had dimensions of 20 mm in diameter and 0.2 mm in thickness. Small disks with diameters of 3 mm were punched from the outer edge of these HPT samples. Thin TEM foils were prepared from the small disks by means of disc grinding, dimpling and finally ion polishing with Ar^+ at an accelerating voltage of 3 kV. The structural characterization was conducted by both JEM-2010 TEM and JEOL 2010F TEM operated at 200 kV.

3 Results and discussion

3.1 General microstructure

Fig.1(a) shows the general deformed microstructure observed in the AA5182 aluminum alloy together with a selected area diffraction (SAD) pattern taken from a 2.54 μm diameter region. The microstructure exhibits grain sizes in the 10–130 nm range and has a very small average grain size of about 55 nm. The grain size distribution is not uniform and grains with different sizes coexist. Dislocation cell structures and subgrains were frequently found inside some larger grains. The misorientation across these cell boundaries increases with further plastic straining, and eventually becomes large enough to transform through low angle grain boundaries (GBs) to high angle GBs [6]. In addition, some GBs in these larger grains are often curved and poorly defined or have a strong spreading of thickness extinction contours (Fig. 1(b)), indicating a high level of internal stresses and elastic distortions in the crystal lattice due to the presence of a local high dislocation density at the boundaries. All of these features suggest that these grains are in a nonequilibrium state having nonequilibrium GBs [6,13].

3.2 Deformation defects

Our previous works confirm that a high density of planar defects was often detected within smaller grains and subgrains with sizes of 20−50 nm [8,19]. The density varies from 10^{16} to 10^{18} m^{-2}. Some of the planar defects were confirmed by HRTEM to be deformation twins and SFs. Fig. 2(a) shows another typical HRTEM image of these defects taken from the subgrain G1 in Fig. 1(b). The width of the subgrain is about 30 nm. The planar defects are indicated by white arrows. It is clearly evident that the planar defects have a habit plane of (111), as the white solid line indicated in Fig. 2(a). The multiple twins and SFs are highlighted in the Fourier-filtered image in Fig. 2(b). These twins are referred to as microtwins or nano-twins since the thickness of the twins spans only 1–4 atomic layers (0.2–1 nm) [19]. Such microtwins and SFs are believed to be formed behind the moving partial dislocations which are emitted from the sub-boundary. The microtwins and SFs were likely heterogeneous nucleates at the sub-boundary and grew larger via the emission of Shockley partial dislocations from the sub-boundary [10]. Therefore, it is reasonable to conclude that the microtwins and SFs observed in Fig. 2 are formed through the heterogeneous mechanism.

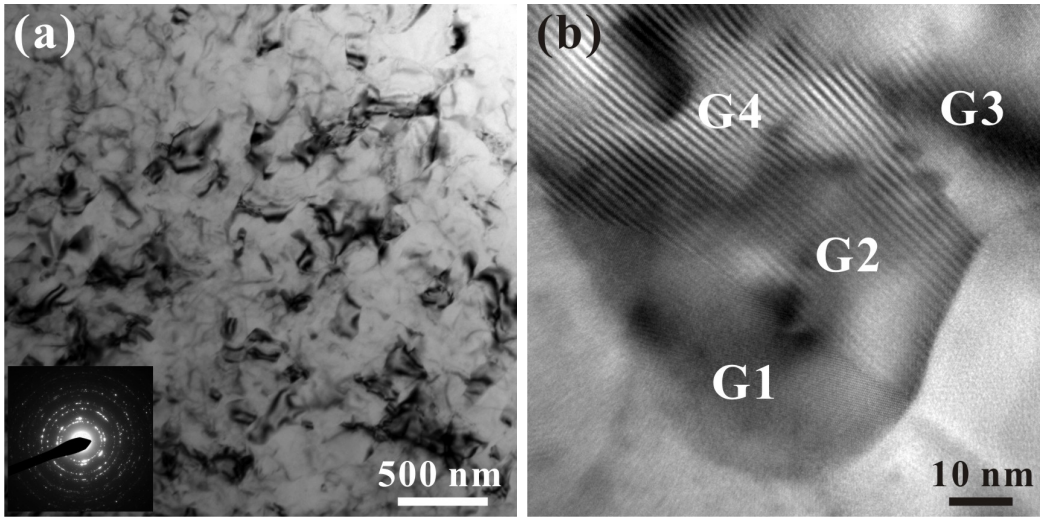

Fig. 1 TEM micrographs of the HPT Al–Mg alloy: (a) bright-field image with a SAD pattern inset; (b) typical grain with nonequilibrium GBs.

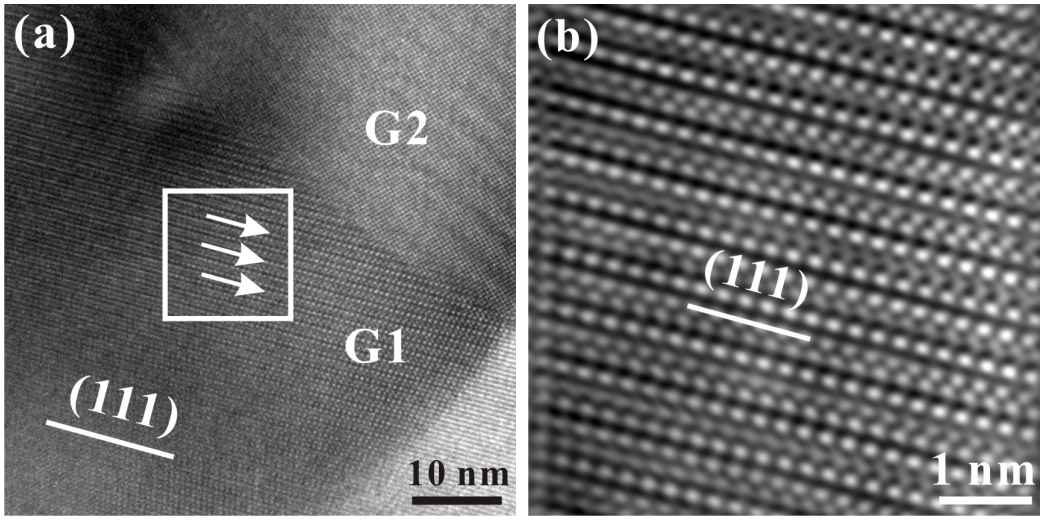

Fig. 2 HRTEM [$1\bar{1}0$] images taken from the subgrain G1 in Fig.1(b): (a) a high density of planar defects lying on (111) plane, indicated by white arrows; (b) inverse Fourier image from the white frame in (a), showing multiple deformation twins and SFs in the subgrain.

Analogous to our previous works on HPT Al–Mg alloys [8,13], a high density of planar defects including SFs and microtwins was frequently detected within both nanocrystalline grains and ultrafine grains in the HPT AA5182 Al–Mg alloy. An example of SFs and microtwins formed within ultrafine grains is shown in Fig. 3(a). Several SFs can be seen inside a 200 nm grain of the alloy. The SF widths are in the range of 5–15 nm and the local SF density is about 2.0×10^{15} m^{-2}. The SFs and microtwins seemed to be preferably located in the vicinity of GBs and sub-boundaries. Therefore, such SFs and deformation twins are believed to be formed behind the moving partial dislocations which are emitted from GBs and GB junctions [10].

It has been suggested that a twin can be formed by the homogeneous mechanism involving the

dynamic overlapping of stacking faults of dissociated dislocations in the grain interiors [10]. Deformation twins formed by such homogeneous mechanism were in fact observed by HRTEM in the HPT alloy. Fig.3(b) shows a deformation twin with a thickness of four atomic planes (about 1 nm). Such a twin was formed by the dynamic overlapping of four SFs of dissociated dislocations on adjacent slip planes. The twin can grow thicker by adding more SFs on either side of the twin.

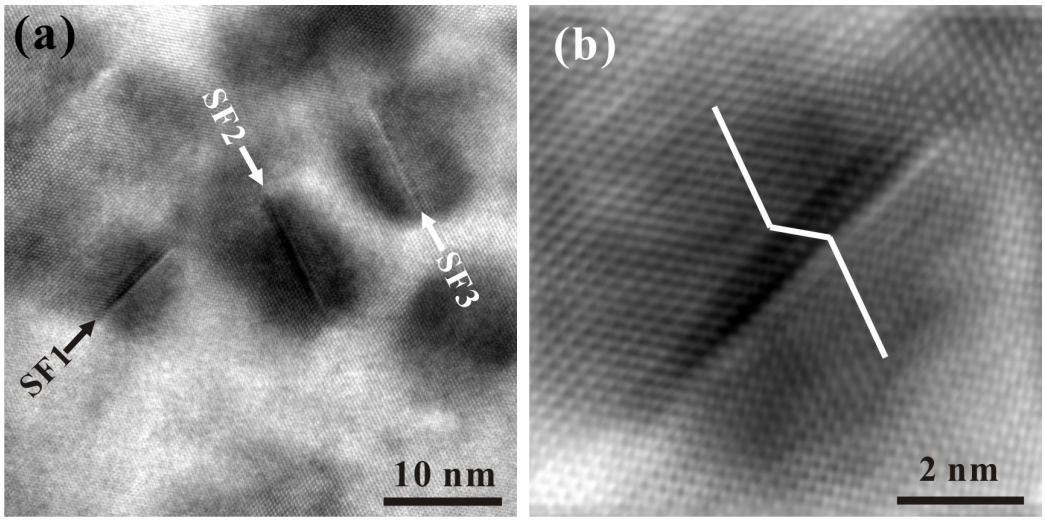

Fig. 3 (a) HRTEM [$1\bar{1}0$] image of a high density of SFs (arrows) and deformation twins within a 200 nm grain in the HPT AA5182 Al–Mg alloy; (b) inverse Fourier image from SF1 in (a), showing a deformation twin with a thickness of four atomic planes (about 1 nm).

3.3 Electron irradiation effect

Both our previous works [6,8,13] and the present observations provide experimental evidence that deformation defects including deformation twins and SFs along the {111} planes can be formed in the HPT aluminum alloys. However Bernhard et al. reported that radiation damage during HRTEM investigations of pure Al and Al alloys can occur [21]. Horita et al. even argued that the lattice defects along the {111} planes in Al and Al based alloys often form (and may disappear) due to the irradiation effect during HRTEM observation [20].

In order to avoid confusion and artefacts and explore the effect of electron beam radiation on the formation of the planar defects, additional HRTEM experiments similar with that of Horita et al. [20] were conducted in the HPT Al–Mg alloy. Fig. 4 shows the structure change of the SFs in Fig.3(a) when keeping the electron beam illumination on the same area of the <110> HRTEM image in Fig.3(a) for some duration of time. As shown in Fig. 4, the SFs in Fig.3(a) gradually disappeared as the duration increased. When the illuminating time reached to 4 minutes (Fig.4(a)), the stacking fault SF1 in Fig.3(a) has disappeared while the stacking faults SF2 and SF3 still existed. Note that the dashed arrows in Fig.4 express the SFs disappear in the locations where the SFs appear in Fig.3(a). As the beam-exposure time increased to 17 minutes (Fig.4(b)), the stacking fault SF2 disappeared but the SF3 was distinguished. All the SFs in Fig.3(a) disappeared completely when the time was 21 minutes (Fig.4(c)). Continuing to increase the time to 28 minutes, there was no any structure change in Fig.4(d) compared to that in Fig.4(c).

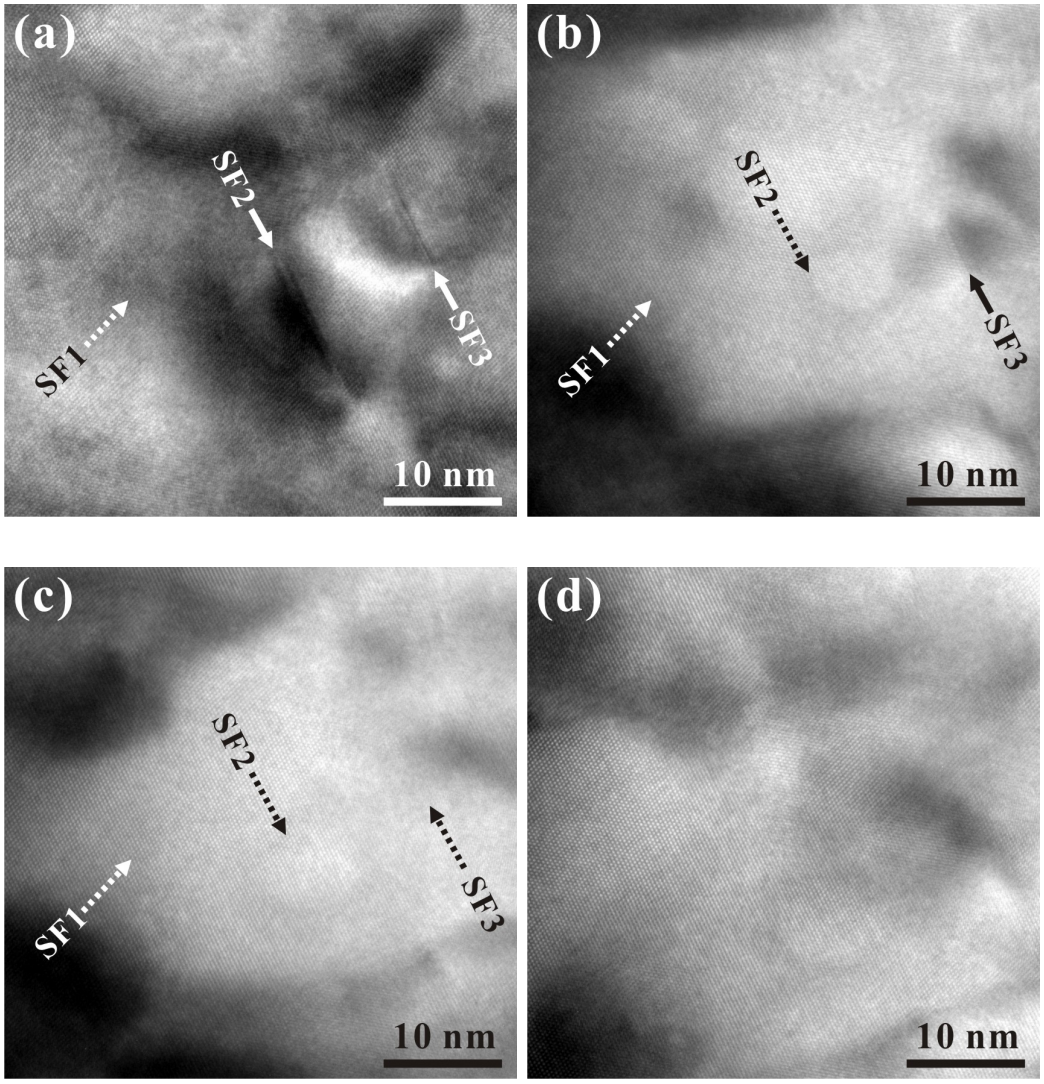

Fig. 4 Disappearance of SFs as the HRTEM image in Fig.3a exposes under the same electron beam illumination with sequential time: (a) 4 minutes; (b) 17 minutes; (c) 21 minutes and (d) 28 minutes. The solid line arrows indicate the SFs still exist as compared with the image in Fig.3a, while the dashed arrows express the SFs disappear in the locations where the SFs appear in Fig.3a.

The results reveal that when a HRTEM image with high densities of SFs exposes under the electron beam for some duration of time, the SFs disappear completely. The possible reasons for this phenomenon during HRTEM observation are probably: (1) Electron beam contamination; (2) Beam radiation / energy. Whether this phenomenon is due to a beam contamination or beam-energy interaction with the defects remains to be clarified. The beam contamination may be the main reason responsible for the SFs disappearance because the local quality of the HRTEM foil probably become bad for getting a clear image of the defects due to the contamination.

Contrary to the results of Horita et al. [20], lattice defects along the {111} planes never appear from a HRTEM image where there are originally no defects due to the beam radiation in the HPT alloy. It seems unlike that these defects will appear within a no-defect area with increasing the beam-exposure time. This postulate has been actually confirmed in Fig.4. Within 28 minutes of the electron illumination, only the

original SFs in Fig.3a disappeared, no other new defects on {111} planes observed in Fig.4 (a)–(d).

In addition, HRTEM $[1\bar{1}0]$ images in areas without any planar defects in the HPT Al–Mg alloy were chosen to further verify the postulate. An example of such HRTEM investigations is shown in Fig.5. Fig.5(a) is the original area and no defects on {111} planes were detected in this area. Keeping the electron beam illumination on the same area in Fig.5 (a) for less than 10 minutes, the structure remained unchanged (Fig.5 (b)–(c)). As the illumination time increased to 30 minutes (Fig.5 (d)), the HRTEM structure has been experienced some changes but no planar defects occurred in the area. Further increasing the time to 60 minutes (Fig.5 (e)), the image kept almost same with that in Fig.5(d). The planar defects haven't appeared even when the beam-exposure time increased to the degree that holes appear in the area (Fig.5 (f)).

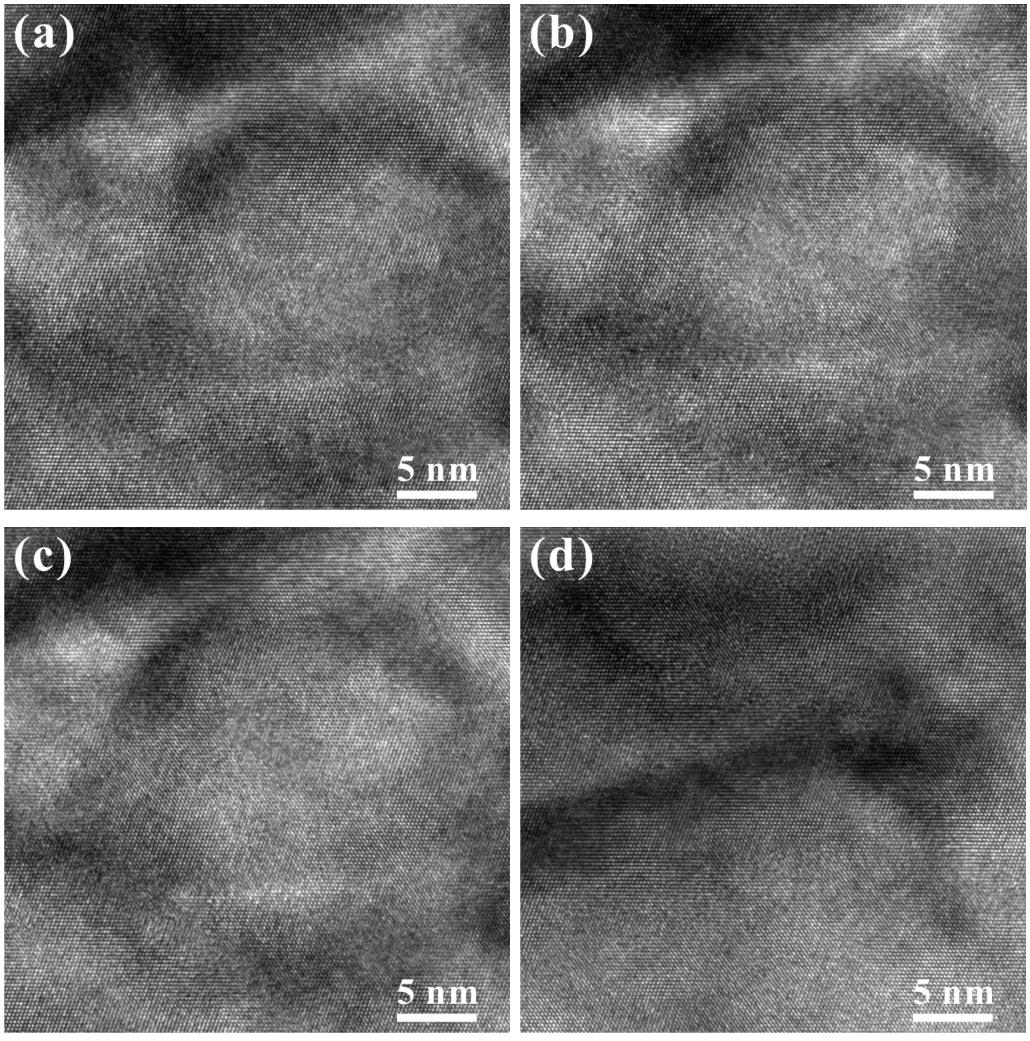

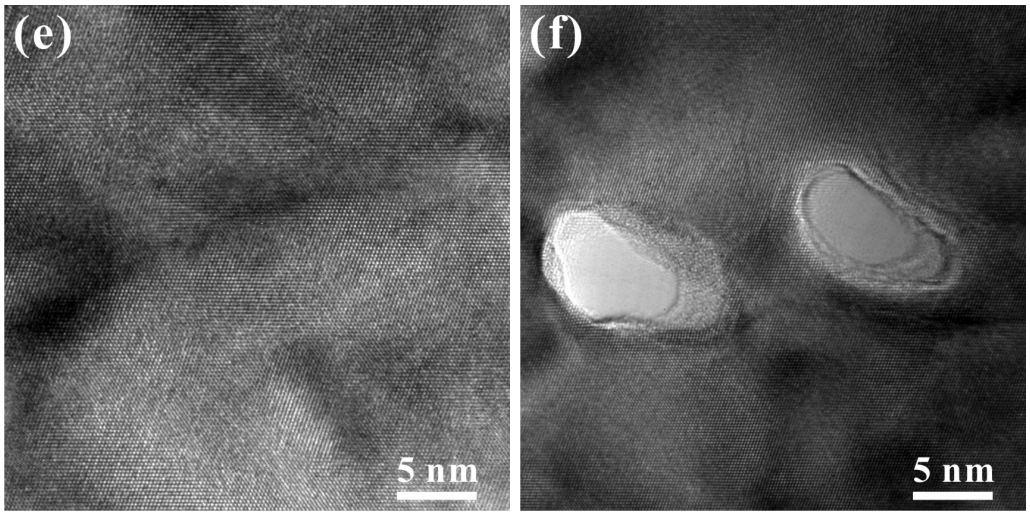

Fig. 5 Structure evolution of an HRTEM [$1\bar{1}0$] image in an area without any planar defects in the HPT Al–Mg alloy exposes under the same electron beam illumination with sequential time: (a) 0 minute; (b) 2 minutes; (c) 6 minutes; (d) 30 minutes; (e) 60 minutes and (f) 120 minutes.

Both the HRTEM examinations in Fig.4 and Fig.5 suggest that the planar defects observed in the SPD alloys are mainly resulted from the significant plastic deformation and are not due to the electron radiation effect during HRTEM observation. The planar deformation defects including SFs along the {111} planes can disappear or become invisible due to electron irradiation or beam contamination but never form in the original areas without planar defects during HRTEM observation. As suggested by Bernhard et al. [21], the planar defects caused by SPD and the radiation defects could be distinguished if they lie on different planes. In fact the deformation defects of the SFs have also been confirmed by HRTEM using <111> beam directions in our HPT Al and Al–Mg alloys. These HRTEM <111> images clearly verify that the deformation defects are formed by the significant plastic deformation in the HPT alloys but these results will be published elsewhere.

It is necessary to note that our HRTEM investigations in this paper only focused on the planar defects in the HPT alloy. The radiation effect on other defects such as point defects is clearly interesting but transcends the scope of the present investigation [21–28].

4 Conclusions

1) Deformation twinning, SFs and partial dislocation emissions from grain boundaries are introduced in the nanostructured Al-Mg alloys. Two twinning mechanisms predicted by MD simulations are verified. A four-layer twin formed by the dynamic overlapping of four stacking faults is observed.

2) The planar deformation defects including SFs along the {111} planes can disappear or become invisible due to electron irradiation or beam contamination but never form in the original areas without planar defects during HRTEM observation.

3) HRTEM examinations confirm that the planar defects of SFs observed in the HPT Al–Mg alloy are mainly resulted from the significant plastic deformation and are not due to the electron radiation effect during HRTEM observation.

4) The radiation effects on other defects such as point defects and dislocations, as well as the interactions between these features in the nanostructure Al-Mg alloys are clearly interesting which need

further investigations.

Acknowledgments

This work was supported by the National Natural Science Foundation of China (grant 50971087), the Basic Research Program (Natural Science Foundation) of Jiangsu Province (grant SBK201222201), the Senior Talent Research Foundation of Jiangsu University (grant 11JDG070), and the Research Council of Norway under the NEW Light Metals of the Strategic Area Materials (grant 10371800). The authors also want to acknowledge the assistance of Dr. Lilya Kurmanaeva (Forschung Center of Karlsruhe, Germany), doing the tensile testing.

References

[1] VALIEV R Z, ZEHETBAUER M J, ESTRIN Y, HÖPPEL H W, IVANISENKO Y, HAHN H, WILDE G, ROVEN H J, SAUVAGE X, LANGDON T G. The innovation potential of bulk nanostructured materials [J]. Adv Eng Mater, 2007, 9(7): 527–533.

[2] VALIEV R Z, ISLAMGALIEV R K, ALEXANDROV I V. Bulk nanostructured materials from severe plastic deformation [J]. Prog Mater Sci, 2000, 45(2): 103–189.

[3] VALIEV R Z, ENIKEEV N A, LANGDON T G. Towards superstrength of nanostructured metals and alloys produced by SPD [J]. Kovove Mater, 2011, 49: 1–9.

[4] VALIEV R. Nanostructuring of metals by severe plastic deformation for advanced properties [J]. Nature Mater, 2004, 3(8): 511–516.

[5] ZHILYAEV A P, LANGDON T G. Using high-pressure torsion for metal processing: Fundamentals and applications [J]. Prog Mater Sci, 2008, 53(6): 893–979.

[6] LIU M P, ROVEN H J, LIU X T, UNGÁR T, BALOGH L, MURASHKIN M, VALIEV R Z. Grain refinement in nanostructured Al–Mg alloys subjected to high pressure torsion [J]. J Mater Sci, 2010, 45, 4659–4664

[7] YAMAKOV V, WOLF D, PHILLPOT S R, GLEITER H. Dislocation-dislocation and dislocation-twin reactions in nanocrystalline Al by molecular dynamics simulation [J]. Acta Mater, 2003, 51(14): 4135–4147.

[8] LIU M P, ROVEN H J, LIU X T, MURASHKIN M, VALIEV R Z, UNGÁR T, BALOGH L. Special nanostructures in Al-Mg alloys subjected to high pressure torsion [J]. Trans Nonferrous Met Soc China, 2010, 20 (11), 2051–2056

[9] ZHU Y T, LIAO X Z, WU X L. Deformation twinning in bulk nanocrystalline metals: Experimental observations [J]. JOM, 2008, 60(9): 60–64.

[10] YAMAKOV V, WOLF D, PHILLPOT S R, GLEITER H. Deformation twinning in nanocrystalline Al by molecular-dynamics simulation [J]. Acta Mater, 2002, 50(20): 5005–5020.

[11] VAN SWYGENHOVEN H, DERLET P M, FRØSETH A G. Stacking fault energies and slip in nanocrystalline metals [J]. Nature Mater, 2004, 3(6): 399–403.

[12] MARIAN J, KNAP J, ORTIZ M. Nanovoid cavitation by dislocation emission in aluminum [J]. Phys Rev Lett, 2004, 93(16): 165503-1–165503-4.

[13] LIU M P, ROVEN H J, MURASHKIN M, VALIEV R Z. Structural characterization by high-resolution electron microscopy of an Al-Mg alloy processed by high-pressure torsion [J]. Mater Sci Eng A, 2009, 503: 122–125.

[14] LIU M P, ROVEN H J, UNGÁR T, BALOGH L, MURASHKIN M, VALIEV R Z. Grain boundary structures and deformation defects in nanostructured Al-Mg alloys processed by high pressure torsion [J]. Mater Sci Forum, 2008, 584/585/586: 528–534.

[15] LIU M P, ROVEN H J, YU Y D. Deformation twins in ultrafine grained commercial aluminum [J]. Int J Mater Res, 2007, 98(3): 184–190.

[16] LIU M P, ROVEN H J, YU Y D, WERENSKIOLD J C. Deformation structures in 6082 aluminium alloy after severe plastic deformation by equal-channel angular pressing [J]. Mater Sci Eng A, 2008, 483-484(1-2 C): 59–63.

[17] ROVEN H J, LIU M P, MURASHKIN M, VALIEV R Z, KILMAMETOV A, UNGÁR T, BALOGH L. Nanostructures and microhardness in Al and Al-Mg alloys subjected to SPD [J]. Mater Sci Forum, 2009, 604-605: 179–185.

[18] LIU M P, ROVEN H J. High density hexagonal and rhombic shaped nanostructures in a fcc aluminum alloy induced by severe plastic deformation at room temperature [J]. Appl Phys Lett, 2007, 90(8): 083115-1–083115-3.

[19] LIU M P, ROVEN H J, MURASHKIN M, VALIEV R Z. Deformation twins and stacking faults in an AA5182 Al-Mg alloy processed by high pressure torsion [J]. Mater Sci Forum, 2008, 579: 147–154.

[20] HORITA Z, SMITH D J, FURUKAWA M, NEMOTO M, VALIEV R Z, LANGDON T G. An investigation of grain boundaries in submicrometer-grained Al-Mg solid solution alloys using high-resolution electron microscopy [J]. J Mater Res, 1996, 97(7): 1880–1890.

[21] BERNHARD M, PETER K. H. Radiation damage during HRTEM studies in pure Al and Al alloys [J]. Int J Mater Res, 2006, 97(7): 1041–1045.

[22] FURUYA K, PIAO M, ISHIKAWA N. High resolution transmission electron microscopy of defect clusters in aluminum during electron and ion irradiation at room temperature [C]// ROBERTSON I M, WAS G S, HOBBS L W. Mater. Res. Soc. Symp. Proc., 1997, 439: 331–336.

[23] KIRITANI M. History, present status and future of the contribution of high-voltage electron microscopy to the study of radiation damage and defects in solids [J]. Ultramicroscopy, 1991, 39: 135–159.

[24] FARRELL K, HOUSTON J T. Suppression of radiation damage microstructure in aluminum by trace impurities [J]. J Nucl Mater, 1979, 83: 57–66.

[25] STURCKEN E F. Irradiation effects in magnesium and aluminum alloys [J]. J Nucl Mater, 1979, 82: 39–53.

[26] MAZEY D J, FRANCIS S, HUDSON J A. Observation of a partially-ordered void lattice in aluminium irradiated with 400 keV Al^{+} ions [J]. J Nucl Mater, 1973, 47: 137–142.

[27] MAZEY D J, BULLOUGH R, BRAILSFORD A D. Observation and analysis of damage structure in Al and Al/Mg (N4) alloy after irradiation with 100 and 400 keV aluminium ions [J]. J Nucl Mater, 1976, 62: 73–88.

[28] MITCHELL D R G. A TEM study of radiogenic silicon precipitation in neutron irradiated aluminium [J]. Nucl Instruments and Methods Phys Res B, 1998, 140: 107–118.